

# A Mechanistic Study of Initiated Chemical Vapor Deposition of Polymers: Analyses of Deposition Rate and Molecular Weight

Kelvin Chan and Karen K. Gleason\*

Department of Chemical Engineering, Massachusetts Institute of Technology, Cambridge, Massachusetts 02139

Received August 10, 2005; Revised Manuscript Received March 24, 2006

**ABSTRACT:** This work studies the effects of changing equilibrium monomer surface concentration on the deposition rates and the number-average molecular weights ( $M_n$ ) of polymers deposited from glycidyl methacrylate and cyclohexyl methacrylate using initiated chemical vapor deposition (iCVD) with *tert*-butyl peroxide as the initiator. Both the surface temperature and the monomer partial pressure were varied to effect different equilibrium surface concentrations, measured using a quartz-crystal microbalance. In either case, the deposition rate and  $M_n$  were found to be linear in equilibrium monomer surface concentration. This strong dependence concludes that chain propagation occurs predominantly on the surface and suggests that the surface concentration is at equilibrium during iCVD, which in turn infers that the adsorption of monomer is not the rate-limiting step in the polymerization process.

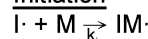
## 1. Introduction

Gas-phase-assisted surface polymerization (GASP) of vaporized vinyl monomers in the presence of initiators has been studied as a method for polymer synthesis. GASP can be used to deposit thin polymer films on surfaces and has a number of advantages over conventional spin-on deposition (SOD). First, surface polymerization does not require the use of solvents and offers environmental benefits for mitigating such use. Second, being a dry method, it allows coatings on nonplanar surfaces and does not have surface tension and nonuniform wetting effects as does SOD, so that complex geometries can be coated. Unlike plasma polymerization, which commonly uses gaseous or vaporized monomers, initiator-assisted surface polymerization involves no plasma discharge, avoiding unnecessary reactions in the gas phase and leading to polymer films of higher quality with well-defined chemical structures that resemble their bulk counterparts. Initiator-assisted surface polymerization can be divided into two categories, pre- and cointroduction, depending on the nature of initiator introduction. In the case of preintroduction, Yasutake and co-workers<sup>1–4</sup> have demonstrated polymerization of vinyl monomers on substrates predeposited with radical initiators, which initiate polymerization of surface-adsorbed monomers to form thin-film polymers. Cointroduction is the process in which both the initiator and the monomer are introduced simultaneously so that no pretreatment of substrates is necessary. Initiated chemical vapor deposition (iCVD) is one such process. In iCVD, initiator and monomer species are vaporized and introduced into a chamber equipped with an array of heated filament wires, suspended several centimeters above the backside-cooled substrate. The purpose of the wires is to thermally dissociate the initiator molecule to create radicals for initiation. This novel setup has been used to deposit a wide variety of polymers such as poly(methyl methacrylate),<sup>5</sup> poly(2-hydroxyethyl methacrylate) and its copolymers,<sup>6</sup> poly(glycidyl methacrylate) (PGMA),<sup>7</sup> poly(tetrafluoroethylene),<sup>8</sup> and fluorocarbon–organosilicon copolymer.<sup>9</sup> Much like conventional free-radical polymerization, iCVD proceeds via four

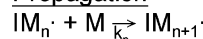
## Radical generation (gas phase/filament)



## Initiation



## Propagation



## Termination

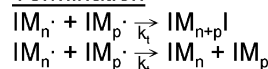


**Figure 1.** Free-radical polymerization scheme.  $I_2$  = initiator,  $I^\cdot$  = initiating radical,  $M$  = monomer, and  $IM_x^\cdot$  = growing radical chain (where  $x$  is any integer).

elementary reaction steps shown in Figure 1. Radical generation is the process of breaking down the initiator molecule into radicals. These radicals in turn initiate the polymerization by attacking the vinyl bonds of the monomer molecules. Propagation proceeds via successive additions of monomer molecules to the growing radical chains. Termination refers to the annihilation of radicals by coupling or disproportionation. Although iCVD and conventional free-radical polymerization, a well-scrutinized subject matter, proceed via the same reaction steps, there are differences between the two warranting further work to understand the iCVD process. In conventional free-radical polymerization, the elementary reactions occur in the same phase with their kinetics determined by a single temperature. In the case of iCVD, there has not been a consensus of where propagation and termination predominantly occur, although radical generation is believed to occur in the gas phase because of the way the heated filament wires are suspended and the substrate is relatively cold.<sup>5–9</sup> The radicals may first travel to the surface before initiation or instead initiate polymerization in the vapor phase. Therefore, initiation, propagation, and termination can occur in the gas phase, on the surface, or both. In contrast, no such uncertainty exists when the initiator is predeposited. The goal of this work is to provide data on surface adsorption of vinyl monomers and to determine the relationship of this adsorption to the overall deposition kinetics

\* To whom correspondence should be addressed: e-mail kkg@mit.edu; Ph (617) 253-5066; Fax (617) 258-5042.

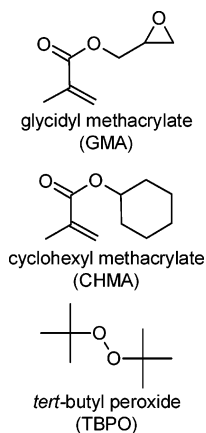


**Figure 2.** Monomers and initiator used in this work.

and the number-average molecular weights ( $M_n$ ) of the iCVD polymeric thin films. Such data will enable conclusions to be drawn as to where the elementary reactions are predominantly occurring. Through increased understanding, polymers of specific properties may be synthesized using iCVD just as they can be with conventional techniques. It is important to realize that this work does not intend to make generalization of all iCVD systems. The exact locations of reactions depend strongly on reaction conditions inside the chamber. The study here serves as a groundwork for increased understanding of iCVD as a method for depositing polymeric thin films.

Two methacrylic monomers and TBPO have been used in this study and are shown in Figure 2. Glycidyl methacrylate (GMA) and cyclohexyl methacrylate (CHMA) were chosen because of their relative ease of iCVD growth and the solubility of their polymers in tetrahydrofuran (THF) for gel-permeation chromatography (GPC). The surface concentration was determined using a quartz-crystal microbalance (QCM), whereas the deposition rate and the molecular weight were determined from iCVD experiments. The surface concentration cannot be determined during iCVD because a polymer film would be deposited on the crystal and make static surface concentration measurement impossible. The surface concentrations measured using the QCM are equilibrium values, but the actual surface concentration during iCVD may or may not be at equilibrium. It must be therefore emphasized that the analysis here is to correlate equilibrium surface concentration to deposition rate and molecular weight. If there is a strong correlation, propagation likely happens predominantly on the surface. The equilibrium surface concentration can be altered via two parameters: the surface temperature and the partial pressure of the species in the vapor phase. In this paper, a section is devoted to the effects of each of these parameters.

## 2. Experimental Section

**2.1. iCVD Experiments.** Films were deposited on 100 mm diameter silicon (Si) substrates in a custom-built vacuum chamber. The inside of the chamber was cylindrical with a height of 3.3 cm and a radius of 12 cm. The inlet of precursor gases and the exhaust were at opposite ends of the chamber. The top of the chamber was covered by a removable quartz plate (~15 cm radius and 2.5 cm thick), allowing placement of substrate, visual inspection, and laser interferometry. The chamber was equipped with a filament array, which provided thermal energy for selective decomposition of molecules. The clearance between the filaments and the stage was 29 mm. The Nichrome filaments (80% Ni/20% Cr, AWG 26, Omega Engineering) were resistively heated to 330 °C, as measured by a thermocouple (Type K, AWG 36, Omega Engineering) directly attached to one of them. The chamber had a backside-cooled stage

**Table 1.** Details of iCVD Experiments

iCVD sample	monomer	sub temp (°C)	flow rate (sccm)			partial press. (mTorr)
			monomer	TBPO	N <sub>2</sub>	
TG1	GMA	25	3.0	1.0	2.0	250
TG2	GMA	30	3.0	1.0	2.0	250
TG3	GMA	35	3.0	1.0	2.0	250
TG4	GMA	40	3.0	1.0	2.0	250
TG5	GMA	45	3.0	1.0	2.0	250
TC1	CHMA	25	2.0	1.0	3.0	167
TC2	CHMA	30	2.0	1.0	3.0	167
TC3	CHMA	35	2.0	1.0	3.0	167
TC4	CHMA	40	2.0	1.0	3.0	167
TC5	CHMA	45	2.0	1.0	3.0	167
PG1	GMA	35	3.5	1.0	1.5	292
PG2	GMA	35	3.0	1.0	2.0	250
PG3	GMA	35	2.5	1.0	2.5	208
PG4	GMA	35	2.0	1.0	3.0	167
PG5	GMA	35	1.5	1.0	3.5	125
PC1	CHMA	35	2.5	1.0	2.5	208
PC2	CHMA	35	2.0	1.0	3.0	167
PC3	CHMA	35	1.5	1.0	3.5	125

on which the substrate was placed and maintained at a constant temperature adjustable between 25 and 45 °C. The chamber pressure was maintained at 500 mTorr with a throttling butterfly valve (Intellisys, Nor-Cal).

The monomers GMA (97.0%+, Aldrich) and CHMA (97.0%, Aldrich) and the initiator TBPO (98%, Aldrich) were used without further purification. GMA liquid was vaporized in a glass jar maintained at  $50 \pm 1$  °C, and this vapor was metered into the chamber through a mass-flow controller (model 1152C, MKS). The CHMA liquid was treated the same way except that the jar was kept at a higher temperature of  $60 \pm 1$  °C. TBPO was maintained at room temperature in a glass jar, and its vapor was metered into the chamber through a different mass-flow controller (model 1479A, MKS). At any time only one monomer was used together with TBPO. Monomer and TBPO vapors were mixed together before entering the chamber through a side port. Depositions were monitored using an interferometry system equipped with a 633 nm HeNe laser source (JDS Uniphase). The cycle thickness was calculated by dividing the actual thickness, as measured using variable-angle spectroscopic ellipsometry (VASE), by the number of cycles. VASE was performed on a J.A. Woollam M-2000 spectroscopic ellipsometer with a xenon light source. Data were acquired at three angles (65°, 70°, and 75°) and 225 wavelengths, and the Cauchy–Urbach model was used to fit the data.

Table 1 details the four sets of iCVD runs in this work. They are divided into two main series: temperature and pressure. In the temperature series, samples were made with the substrate temperature varied between 25 and 45 °C and other parameters fixed. Samples TG and TC are two sets of such samples. In the pressure series, samples were made with varying monomer partial pressure and other parameters were held fixed. Samples PG and PC are two sets of such samples. It should be noted that in the pressure series the total flow rate was kept constant with a patch flow of nitrogen (N<sub>2</sub>) while the monomer flow rate was varied. This setup was to maintain the same residence time for all runs. The total flow rate (6 sccm), the filament temperature (330 °C), and the chamber pressure (500 mTorr) were the same for all 18 samples in Table 1. For each of the iCVD runs, the flow rates and the chamber pressure were allowed time to stabilize before voltage was supplied to the filament wires. All samples were grown to an approximate thickness of 1.3 μm.

Films were dissolved in tetrahydrofuran (THF) for GPC measurements. The GPC system was comprised of a Waters 1515 isocratic high-performance liquid chromatography (HPLC) pump, a Waters 2414 refractive index detector, and two Styragel HR 4  $7.8 \times 300$  mm columns. Poly(methyl methacrylate) (PMMA) standards (Polymer Laboratories, Amherst, MA) dissolved in THF were used for calibration at 35 °C.

**2.2. Quartz-Crystal Microbalance Measurements.** A quartz-crystal microbalance (QCM, model VSO-100) with a 14 mm diameter gold-coated quartz sensor crystal (model 500-117) was obtained from Sycon Instruments (Syracuse, NY). It was placed inside the iCVD chamber described in section 2.1 and was actively cooled or heated with temperature-controlled water. The QCM output its signal to a board monitor (model STM-1, Sycon) through industry-standard coaxial cables via a filter (model OSC-100A, Sycon). The board monitor was connected to a Windows-based computer through its RS-232 interface with USB interface conversion. Software supplied by Sycon installed on the computer monitored the thickness of material on the sensor crystal.

The QCM was used to obtain surface monomer concentration data. The software was configured to output the thickness of material. Thicknesses in angstroms were converted to normalized monomer surface concentrations, [M], in arbitrary units using eq 1. This normalization is a conversion from the thickness to a quantity representative of the number of molecules on the surface. The reference thickness is taken to be the lowest thickness obtained in this work for GMA (reference molecular weight = 142.15 g/mol).

$$[M] = \frac{d}{FW} \bigg/ \frac{d_r}{FW_r} \quad (1)$$

where [M] = monomer surface concentration (in au),  $d$  = thickness (in Å),  $FW$  = formula weight of monomer (in g/mol),  $d_r$  = reference thickness (5.41 Å), and  $FW_r$  = reference formula weight (142.15 g/mol).

Eighteen different QCM measurements were done to mimic the iCVD conditions listed in Table 1. The only differences between the corresponding QCM conditions were that TBPO was replaced with nitrogen and the filaments were off. For instance, the corresponding QCM measurement for iCVD sample TG1 in Table 1 was performed with a QCM temperature of 25 °C, a GMA flow rate of 3.0 sccm, a nitrogen flow rate of 3.0 sccm, and a total pressure of 500 mTorr. The flow rates and the total pressure were allowed time to stabilize before the QCM was turned on. When the thickness measured by the QCM stabilized at a constant value, data logging was started and the nitrogen flow rate was increased to 6.0 sccm. Immediately after the flow of nitrogen was increased, the monomer flow was stopped, so that the only species flowing through the chamber was nitrogen. This procedure purged the reactor with nitrogen while maintaining the total pressure at 500 mTorr. The monomer molecules that were previously adsorbed onto the QCM desorbed from the surface because the monomer partial pressure decreased to zero due to purging, causing the measured thickness to decrease. When the thickness stabilized and stopped fluctuating, data logging was halted. The difference between the final and the initial thicknesses corresponds to the amount of monomer that was desorbed from the sensor crystal and represents the equilibrium monomer surface concentration under the conditions before the nitrogen flow was increased and the monomer flow was stopped. The thickness differentials were converted to surface concentrations using eq 1.

### 3. Results and Discussion

**3.1. Changing Surface Temperature.** Figure 3 shows the QCM data of equilibrium surface concentration as a function of surface temperature. Everything but the crystal temperature was fixed in these measurements. The crystal temperature was varied between 25 and 45 °C in 5 °C increments. The partial pressures of GMA and CHMA were fixed at 208 and 167 mTorr, respectively. These pressures were chosen to avoid condensation at 25 °C and to match those of iCVD experiments (series TG and TC in Table 1). As seen from Figure 3, the equilibrium surface concentration increases with decreasing surface temperature in a nonlinear manner.

iCVD experiments were run with the same conditions used for the QCM measurements. The design was to keep the partial

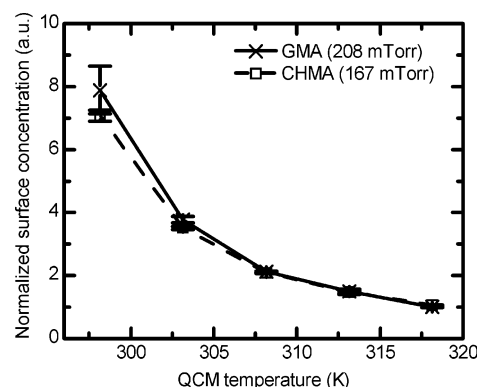


**Figure 3.** Equilibrium monomer surface concentration as a function of surface temperature as measured by the quartz-crystal microbalance (QCM). The partial pressure of GMA was fixed at 208 mTorr for the experiment, while that of CHMA was set at 167 mTorr.

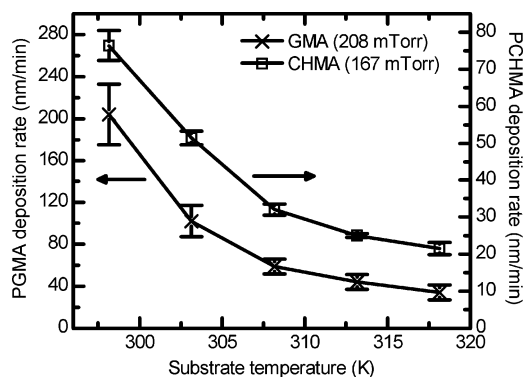


**Figure 4.** Deposition rate as a function of substrate temperature. The partial pressure of GMA was fixed at 208 mTorr, while that of CHMA was maintained at 167 mTorr.

pressure of the monomer in the gas phase constant while varying the substrate temperature but holding all other reactor settings constant. In the gas phase, initiator molecules are broken down into initiating radicals, and it is assumed that the change in substrate temperature does not affect the gas temperature. Therefore, the kinetics of radical generation and the gas-phase concentration of the initiating radicals stayed constant in both the TG and the TC series. This assumption is justified because of two reasons. First, the measured filament temperature has never been observed to decrease when lower substrate temperatures are used. Second, the heat transfer between the gas phase and the surface at the conditions during iCVD at a vacuum pressure of 500 mTorr is estimated to be poor using the forced convection equation developed for flow parallel to planar surfaces.<sup>10,11</sup> Thus, the gas-phase temperature, in addition to the gas-phase concentrations, remains constant throughout the TG and TC series.

Mao and Gleason reported that, when the filament temperature was high, smooth films with rms roughness of 0.30 nm could be made.<sup>12</sup> The same conditions of high filament temperature were applied to this work to avoid surface roughening, which causes the deposition rate to be unsteady. Figures 4 and 5 show the deposition rate and the molecular weight, respectively, as functions of substrate temperature. Both quantities increase with decreasing substrate temperature. Not only do these quantities follow the same trend as the equilibrium surface concentration, they also provide the same nonlinear response as observed in Figure 3. This can be seen explicitly by plotting deposition rate and number-average molecular weight,  $M_n$ , directly against the equilibrium surface concentration. These graphs can be made because both the deposition

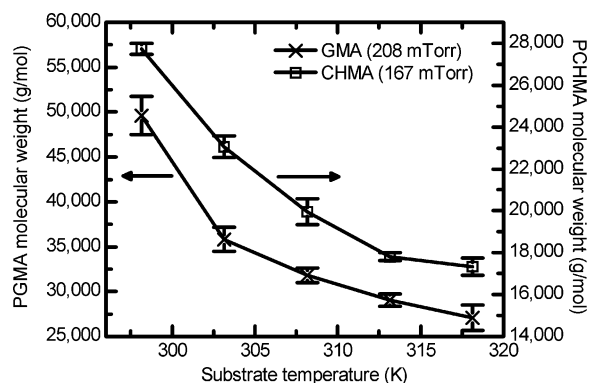


**Figure 5.** Number-average molecular weight as a function of substrate temperature. The partial pressures of GMA and CHMA were set at 208 and 167 mTorr, respectively.

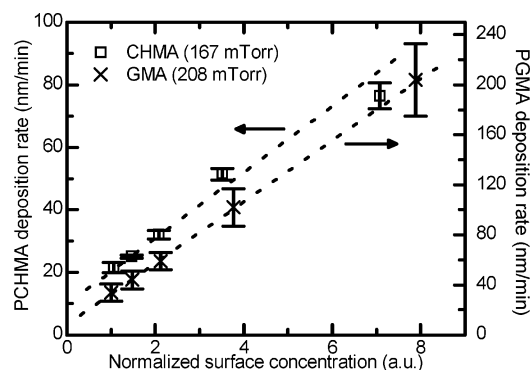


**Figure 6.** Plot of deposition rate data from iCVD experiments against equilibrium surface concentration data from QCM measurements. For each of the monomers, the iCVD and the QCM data were collected at the same monomer partial pressure.

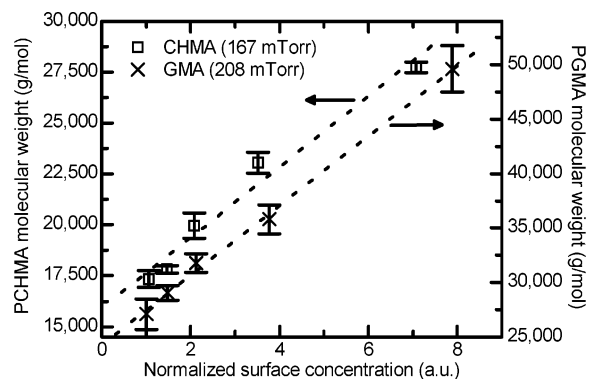


**Figure 7.** Plot of number-average molecular weight from GPC measurements on dissolved iCVD polymer films against equilibrium surface concentration data from QCM measurements. The iCVD and the QCM experiments had matching monomer partial pressures.

and the QCM experiments were designed to have matching conditions—the partial pressure of the monomer, the total pressure, and the total flow rate were identical. The common variable was the surface temperature. Figures 6 and 7, which plot the deposition rate and  $M_n$ , respectively, against equilibrium surface concentration, both show a linear relationship. Each data point is the average of three measurements, and the  $R^2$  values of the linear fits are all higher than 0.97.

The positive linear correlation of growth rate and molecular weight on surface concentration at fixed gas phase temperature and concentration is consistent with chain propagation occurring predominantly on the surface and inconsistent with the alternate hypothesis of gas phase propagation. Indeed, lowering the substrate temperature would promote adsorption of any chains

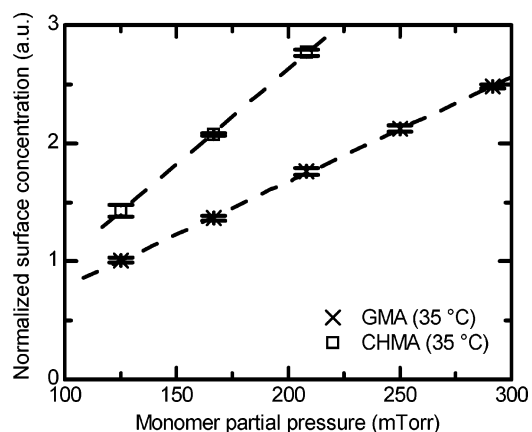


**Figure 8.** Normalized surface concentration as a function of monomer partial pressure. Both sets of measurements were performed at a crystal temperature of 35 °C.

propagated in the gas phase, which could account for the observed increase in growth rate. However, lowering substrate temperature would increase the condensation of the more volatile shorter chain species, resulting in a decrease in molecular weight. Exactly the opposite is observed: lowering substrate temperature increases molecular weight. Additionally, propagation in the gas phase would require bimolecular gas-phase reactions at vacuum pressure of hundreds of milliTorr. The corresponding gas-phase concentrations of  $\sim 10^{-5}$  M limit the probability of the third body collision required for conservation of energy.<sup>13</sup> Finally, the volatility of species containing more than one monomer unit is very low. (A growing chain with two monomer units has a molecular weight of over 350 g/mol.) Altogether these facts strongly support the hypothesis that propagation occurs predominantly on the surface, and the increase in deposition rate and molecular weight can be attributed to the increase in surface concentration of monomer as surface temperature decreases.

The observation that the deposition rate and  $M_n$  align well with the equilibrium surface concentration as measured by the QCM signifies that the surface monomer concentration is likely at equilibrium with its gas-phase concentration during actual deposition. Such an equilibrium indicates that iCVD is not monomer adsorption limited, and the process is subject to some other limitation (e.g., the arrival of initiating radicals by mass transport through the gas phase or the propagation rate kinetics). A rate-limiting step is often encountered in heterogeneous reaction systems.<sup>14</sup>

**3.2. Effects of Monomer Partial Pressure on Deposition Rate and Molecular Weight.** The discussion here is extended to changing surface concentration through manipulation of the partial pressure. Figure 8 shows that the equilibrium surface concentrations of both monomers, as measured by the QCM, increase linearly with increasing monomer partial pressure. At any given monomer partial pressure, the surface concentration of CHMA is higher than that of GMA, consistent with the fact that CHMA is heavier than GMA.

For the iCVD runs in series TG and TC (Table 1), the temperature was altered to manipulate surface concentration. Here in series PG and PC, the partial pressure was varied to effect different surface concentrations. The design was to keep the surface temperature constant while varying the monomer partial pressure but keeping all other parameters constant. As with the temperature series, the deposition rate and the number-average molecular weight data are plotted against the equilibrium surface concentration data, shown in Figures 9 and 10.

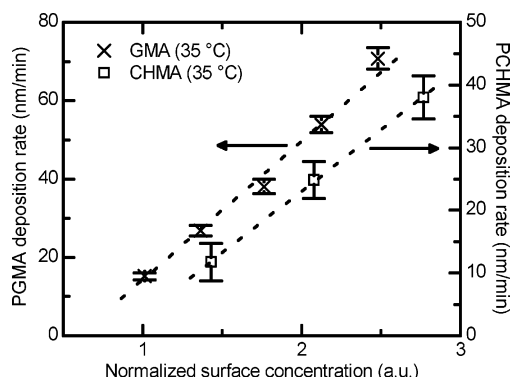


**Figure 9.** Deposition rate from iCVD experiments as a function of normalized surface concentration from QCM measurements.

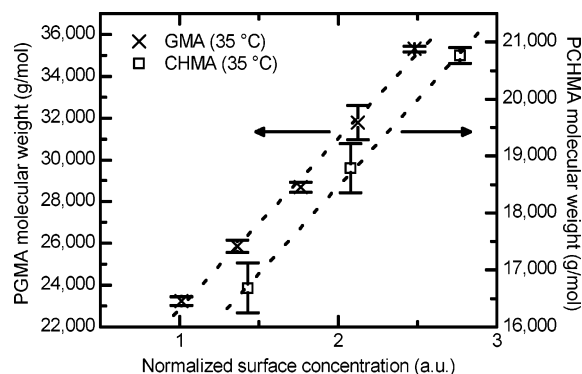


**Figure 10.** Number-average molecular weight as a function of normalized surface concentration from QCM measurements.

For each of the monomers, the deposition rate and the number-average molecular weight display a linear increase with increasing surface concentration, providing additional support that propagation occurs predominantly on the surface.

One can see that at any given surface concentration the iCVD of PGMA has a higher deposition rate and a high molecular weight. The slopes of the fitted lines of the GMA series in Figures 9 and 10 are 37.2 nm/(min au) and 8120 g/(mol au), respectively, compared to 19.7 nm/(min au) and 3051 g/(mol au) for CHMA. The difference in deposition rates is wider than the difference stemming from the disparity between the molecular weights of the monomers (i.e., per unit thickness there are more GMA than CHMA units). The consistently higher slopes for GMA may stem from the difference(s) in kinetic parameters. The dominant difference is likely in the termination rate coefficient,  $k_t$ , because the propagation rate coefficients for both GMA and CHMA are similar according to the literature based on PLP-SEC (pulsed laser polymerization-size exclusion chromatography) experiments.<sup>15</sup> Based on radical chain algebra for free-radical polymerization,<sup>16-18</sup> both the rate of polymerization and chain length are inversely proportional to the square root of the termination rate coefficient. To use the results in Figures 9 and 10 to estimate the difference between the termination rate coefficients of the two monomers, the units in the figures must be converted. To convert thickness per unit time into number of moles per unit area per unit time, a density of 1 g/cm<sup>3</sup> is assumed for both polymers. To convert number-average molecular weight into number of repeat units, the  $M_n$  is simply divided by the formula weight of the each respective monomer. After conversion, the ratio between the polymeriza-

tion rates (in number of moles per unit time per unit area) of GMA and CHMA is 2.2, and that between the chain lengths (in number of repeat units) of GMA and CHMA is 3.2. Based on the inversely proportional relationship, the squares of these numbers equal the ratios between the termination rate coefficients of CHMA and GMA. The  $k_t$  of CHMA is therefore 5.0 and 9.9 times greater than that of GMA based on results from Figures 9 and 10, respectively. The mismatch between the numbers is likely due to experimental imprecision. The higher  $k_t$  of CHMA leads to slower deposition and lower molecular weight.

#### 4. Conclusions

This work shows that chain propagation occurs predominantly on the surface of the substrate for the iCVD of PGMA and PCHMA. The fact that the molecular weight increases with decreasing substrate temperature is a strong support of the hypothesis of a surface mechanism for the propagation step of the polymerization. The linearity between the deposition rate and the molecular weight data from iCVD experiments and the equilibrium surface concentration data from QCM measurements shows that the kinetics of polymerization depends strongly on the equilibrium surface concentration. This dependence infers that the surface concentration is at equilibrium during iCVD and that the rate-limiting step is not the adsorption of monomer. The inherently slow deposition and low molecular weight of iCVD PCHMA are likely due to faster termination kinetics.

**Acknowledgment.** The authors acknowledge the support of the NSF/SRC Engineering Research Center for Environmentally Benign Semiconductor Manufacturing.

#### References and Notes

- (1) Yasutake, M.; Hiki, S.; Andou, Y.; Nishida, H.; Endo, T. *Macromolecules* **2003**, *36*, 5974.
- (2) Yasutake, M.; Andou, Y.; Hiki, S.; Nishida, H.; Endo, T. *J. Polym. Sci., Polym. Chem.* **2004**, *42*, 2621.
- (3) Yasutake, M.; Andou, Y.; Hiki, S.; Nishida, H.; Endo, T. *Macromol. Chem. Phys.* **2004**, *205*, 492.
- (4) Andou, Y.; Yasutake, M.; Jeong, J. M.; Nishida, H.; Endo, T. *Macromol. Chem. Phys.* **2005**, *206*, 1778.
- (5) Chan, K.; Gleason, K. K. *Chem. Vap. Deposition* **2005**, *11*, 437.
- (6) Chan, K.; Gleason, K. K. *Langmuir* **2005**, *21*, 8930.
- (7) Mao, Y.; Gleason, K. K. *Langmuir* **2004**, *20*, 2484.
- (8) Pryce Lewis, H. G.; Caulfield, J. A.; Gleason, K. K. *Langmuir* **2001**, *17*, 7652.
- (9) Murthy, S. K.; Olsen, B. D.; Gleason, K. K. *Langmuir* **2002**, *18*, 6424.
- (10) Welty, J. R.; Wicks, C. E.; Wilson, R. E. *Fundamentals of Momentum, Heat, and Mass Transfer*, 3rd ed.; Wiley: New York, 1984.
- (11) Geankoplis, C. J. *Transport Processes and Unit Operations*, 3rd ed.; Prentice Hall: Englewood Cliffs, NJ, 1993.
- (12) Mao, Y.; Felix, N. M.; Nguyen, P. T.; Ober, C. K.; Gleason, K. K. *J. Vac. Sci. Technol. B* **2004**, *22*, 2473.
- (13) Butt, J. B. *Reaction Kinetics and Reactor Design*, 2nd ed.; Marcel Dekker: New York, 2000.
- (14) Fogler, H. S. *Elements of Chemical Reaction Engineering*, 3rd ed.; Prentice Hall: Upper Saddle River, NJ, 1999.
- (15) Beuermann, S.; Buback, M.; Davis, T. P.; Garcia, N.; Gilbert, R. G.; Hutchinson, R. A.; Kajiwar, A.; Kamachi, M.; Lacik, I.; Russell, G. T. *Macromol. Chem. Phys.* **2003**, *204*, 1338.
- (16) Odian, G. G. *Principles of Polymerization*, 3rd ed.; Wiley: New York, 1991.
- (17) Rodriguez, F. *Principles of Polymer Systems*, 4th ed.; Taylor & Francis: Washington, DC, 1996.
- (18) Kumar, A. S.; Gupta, R. K. *Fundamentals of Polymers*; McGraw-Hill: New York, 1998.

MA051776T